energies

MDPI

Article

Energy Performance Assessment of the Container Housing in Subtropical Region of China upon Future Climate Scenarios

Hua Suo [1], Xinxin Guan [2], Shanglin Wu [1] and Zhengyu Fan [3,*]

[1] College of Transportation Engineering and Architecture, Foshan University, Foshan 528225, China
[2] Guangzhou Branch, Shenzhen Architectural Design Institute, Guangzhou 510499, China
[3] College of Architecture, Xi'an University of Architecture and Technology, Xi'an 710055, China
* Correspondence: fanzhengyu@xauat.edu.cn; Tel.: +86-13020288595

Abstract: Being continuously abandoned in huge amounts year-round by freight industry, shipping containers meet increasing regenerative utility in forms of temporary buildings, small public facilities, etc., especially in fast-developing countries with large populations and high living intensities like China. Although recycled containers have been nicely entitled with green building visions, their characterized inferior thermal properties (low inertia, poor insulation, etc.) when compared to conventional building forms and materials will greatly hinder their energy-saving potential, especially under the serious future extreme climate expectations. It therefore becomes particularly necessary to uncover the actual energy and thermophysical behaviors of the container building typology, upon extreme future climate scenarios targeting zero carbon forms for small-scale and temporary buildings in the upcoming future. In reference to existing data, this study made reasonable predictions of future extreme climate conditions (2050 and 2080), employing the Morphing method, and examined the cooling energy performances of the typical container housing in a subtropical climate through dynamic simulations. The energy-saving effectiveness of key design variables including insulation types, thicknesses, window opening areas and air infiltration rates has been validated and quantitatively revealed for such a building typology among the tested hot summer and warm winter region. Results imply that the additional energy burden brought by future extreme weather conditions cannot be ignored. The heat gains from envelopes and hot air infiltration are both key design factors of cooling energy increments for such building types upon future extreme climates. Compared with expanded pearl- and vermiculite-type insulation materials, thinner (70~90 mm) plastics and mineral wool-type ones have better energy-saving performance and therefore are worth consideration. High air infiltration rates and window openings in eastern or western orientations shall be carefully selected. The research outcomes can provide key references for design decisions made for the energy-efficient and low-carbon design of the container building typology among subtropical zones, or similar climate regions in response to future climate conditions.

Keywords: container; climate change; future climate; energy performance; energy efficiency

Citation: Suo, H.; Guan, X.; Wu, S.; Fan, Z. Energy Performance Assessment of the Container Housing in Subtropical Region of China upon Future Climate Scenarios. *Energies* **2023**, *16*, 503. https://doi.org/10.3390/en16010503

Academic Editor: Luisa F. Cabeza

Received: 15 November 2022
Revised: 28 December 2022
Accepted: 28 December 2022
Published: 2 January 2023

1. Introduction

Compared with traditional forms, buildings with recycled freight containers as carriers maintain not only lower costs but also more abundant material resources. In China, the annually shipped containers throughout 2019 alone had reached 261 million twenty feet equivalent units (TEU) [1]. Even when considering the safety regulation by the freight industry (max. life expectancy of most containers is only 10–15 years), unlike conventional buildings the container typology has enjoyed increasing popularity as a new form of small volume urban buildings due to its obvious advantages and relative suitability in capacity, strength and cost, etc. Huge numbers of temporary buildings, public facilities and modular collective housing carried by container units have been built at a high speed among urban areas globally.

Taking the epidemic restriction situation in China for instance, since the outbreak of the global epidemic in 2020, countless transit, detection, isolation, residential modules or centers have been built with containers as the basic unit carrier. Throughout the epidemic-prevention activities of Wuhan City, only the Huoshenshan shelter hospital has employed more than 600 containers for construction [2]. Throughout all major cities around China or even worldwide, thousands of nuclein detection points have also been deployed in form of freight containers (Figure 1).

(**a**) (**b**) (**c**) (**d**) (**e**)

Figure 1. Shelter hospital/nuclein detection points in container carriers deployed in (**a**) Shanghai; (**b**) Guangzhou; (**c**) Xi'an; (**d**) Hohohot; (**e**) Dalian.

Other than these, architects and designers have also tried to expand its potential as carriers of various public functions. Most such experiments still adopt the original units in small scale. James & Mau had combined two 40-foot containers together with two 20-foot containers to create the Manifesto House as a new small-scale housing type with all envelopes refurbished by sustainable biomasses [3]. Some quite famous practices also made use of container units in a collective manner, including the "Container City" built by Erik Reynolds for the British Urban Space Organization at London Pier [4], the Keetwonen student dormitory designed and built by the Dutch Tempohousing Office in Amsterdam [5], and the reconstituted post-earthquake housing proposed by Shigeru Ban in Miyagi-ken, Japan [6].

More recently, the 2022 FIFA World Cup holder country Qatar has finished the so-called "Stadium 974", constructed from 974 containers in Doha for the grand event. They even accommodated visiting fans with 6000 cabin rooms newly built from containers [7,8]. Simultaneous needs of more flexible urban emergency services, more diverse public facility types, more convenient construction processes, and more comfortable built environments among modern cities have led to the development of container carrier building forms to a new phase and have also triggered some quite urgent practical problems.

On the other hand, due to emerging global issues, including excessive global emissions, greenhouse effects, and energy crisis, the escalating building energy consumption becomes more critical for future urban livings. It is therefore an inevitable trend to realize the worldwide up-scaling of nearly zero- or zero-energy buildings. For example, in China, a country maintaining the largest total energy consumption and almost 1/3 of all greenhouses gas (GHG) emissions on this planet [9], the building sector has already contributed to 46.5% of national energy consumption and 51.2% of national carbon emissions [10]. The Chinese central government has therefore enforced a wide range of incentives and policies related

to building energy efficiencies, and in 2020 the country announced its ambition to be carbon-neutral by 2060 [11].

However, the proportion and corresponding importance of container carrier-resulted energy consumption among the total amount of urban building sector has kept growing to be an increasingly noticeable part. In fact, a great many integration practices harvesting various renewable energy resources (solar, wind energy etc.) have experimented with container carriers, shaping the building form to be an ideal blueprint for near zero- and zero-energy consumption buildings [12–17].

Within such a context, however, an understanding of the heat gain and energy consumption performances of container carrier type buildings was still very limited, as most thermal and energy efficiency research was conducted with a focus on more commonly seen building forms. Due to their relatively larger area proportion and featured properties (high heat transfer coefficient, low thermal inertia, etc.) of envelopes, container carrier buildings actually have higher heat exchange efficiency with the outsides and thus are more sensitive to external disturbances [12].

Meanwhile, climate change has become a globally recognized fact. The Intergovernmental Panel on Meteorological Change (IPCC) has reported that, compared with pre-industrialization human activities were estimated to have caused about 1.0 °C global warming, and the global average surface temperature observed from 2006 to 2015 was 0.87 °C higher than the 1850–1900 average. In view of the long-term warming trend, based on the current heating rate, global warming may reach 1.5 °C from 2030 to 2052 [18,19]. Upon current global temperature rises, the even hotter summer and colder winter have further increased the annual building energy burden. As mentioned above, container carrier buildings are comparatively even more sensitive to harsh external environments, and the corresponding deterioration of thermal environment and energy consumption is likely to be more severe. The demand of indoor thermal and energy performance improvements against future climate change becomes more prominent.

In this context, it is urgent and important to explore feasible optimization pathways to enhance the energy performance of container carrier buildings in response to future climate conditions. In particular, reasonable thermal constructions of the container envelopes could be the critical point to ensure total energy consumption control and to achieve nearly zero- or zero-energy prototypes for future small scale building modules within urban areas globally.

2. Literature Review

To date, quite some research works have been carried out to investigate the physical performances or built environments of container buildings. However, most such optimization studies were carried out in accordance with the previous meteorological data experiences.

Many of these studies are devoted to demonstrating the feasibility of realizing near zero-energy or zero-energy buildings through on-site renewable energy utilization around the containers. S. Schiavoni et al. reported their attempt of designing nearly zero-energy buildings using abandoned shipping containers named HPP, as located in Perugia (central Italy) for either forestry, emergency, or low-cost housings. Employing EnergyPlus, SimaPro, and DIALux, respectively, they analyzed the energy, environmental, and lighting performances of typical container carried housings in varies sizes, and proved the possibility to achieve nZEB with a container house type [20]. With the aid of TRNSYS simulation and a real demonstration prototype in Shanghai (China), A. B. Kristiansen, together with his research group, had investigated the feasibility of achieving off-grid container units based only on solar energy resource. The shortage in heating energy supply has been evidenced among such hot summer and cold winter climates [21]. They also performed energy analyses and lifecycle assessments for container buildings in varied designs and evidenced the lowest lifecycle impacts of net-zero energy design in all categories [22]. M. Trancossi et al. proposed an innovative heat pump that couples both solar

and thermoelectric contributions and evaluates their implementation performance in an energy-efficient container house, while also considering the weather of Bologna (Italy). It was pointed out that there were three qualifying elements of a well-performed design: sandwich walls include vacuum-insulated panels (VIPs) for minimizing heat dispersions, seasonal shading evaluation-based optimized smart windows, and an innovative cogeneration heat pump based on thermoelectric effect with heat recovery from photovoltaic systems [23].

Some research also focused on the design optimization of container buildings for enhanced energy or indoor thermal performances in specific climates.

A. M. Tanyer et al. examines the airtightness performance of four types of commonly used container houses and their corresponding energy efficiencies upon the climate of Ankara (Turkey). They proved that the airtightness level exhibits as a critical point for the overall energy performance of the container building, and sealing the interior surfaces of junctions and edges can improve the airtightness level considerably [24]. H. Taleb et al. pointed out that, for container homes in a subtropical desert area (Aswan, Egypt), having green skin as the insulation layer for the container envelope played a key role in reducing the local cooling load [25]. X. Nan et al. also confirmed that the indoor thermal performance of containers could be steadily improved in winter by external living wall systems (LWSs) among Hangzhou (China)-represented regions with wet and cold winter climates [26]. M. L-Pelaez and his coworkers at the Massachusetts Institute of Technology presented their validation work over an EnergyPlus model of a hydroponic container farm in Boston (U.S.), based on nine months of measured data. Results show that through representing plant–air interactions within EnergyPlus and modeling the cooling coefficient of performance as a function of outdoor air temperature, one can reliably predict annual container farm energy use [27]. Through case studies in Nordic (Stockholm, Sweden), Central-European (Berlin, Germany) and Tropical (Addis Ababa, Ethiopia) climates, respectively, J. Koke et al. proposed the application of their design strategies and energy systems in Nearly Zero-Energy Container Buildings (NZECBs) among different climates. It has been shown that the NZECB goal (self-sufficiency rates up to 80%) can be achieved through the use of wall constructions with VIPs and phase-change materials (PCMs) as well as various renewable energy systems consisting of PV, solar thermal, battery storage, and air/geothermal heat pumps, etc. [28].

Only very limited studies have considered the risk of climate change and conducted research over the performance response of a similar volume of containers upon future climate scenarios.

Fabrizio A. et al. examined the resilience to climate change in the aim of nearly zero energy-buildings designed according to the EPBD recast through experimental monitoring and simulations of a container-like real case model named BNZEB, located in Benevento (southern Italy) with a Mediterranean climate [19]. They found that, upon a medium-term climate projection, the reduction of the heating demand could compensate the increment in the cooling request, and the occupants will require a higher number of operating hours with more frequent switching on and off.

It can be seen that almost all existing work carried out considers past climate experiences, even for future-oriented nNEB or NEB design optimizations of container buildings. Far too little work has explored how the actual building performance, especially the energy behaviors of containers, will react to upcoming climate deterioration, and the optimization measures, potentials of energy efficiency accordingly.

Meanwhile, among the proven optimization design methods for container buildings, the measures to fit the subtropical region's needs are relatively limited. Not only do VIP and PCM technologies demand relatively high costs, LWS is also not universally applicable. In the face of the coming construction needs in larger scales among this region, more practical, economical, and widely applicable design choices are urgently needed to be validated.

In such a context, it become necessary to study the thermal and corresponding actual energy performances of container-type building in subtropical climates upon the remodeled

extreme climate scenario predictions to ensure the real low-carbon or zero-carbon basis for such small-scale housing types in the coming future.

Through this study, the thermophysical and energy performance of the typical freight container housing modeled in Guangzhou city (Southern China) has been evaluated by means of dynamic simulations, upon the present Typical Meteorological Year (TMY) and generated future climate scenarios of 2050 and 2080. Accordingly, energy-saving strategies based on appropriate insulation types, thicknesses, window-to-wall ratios, and infiltration rates have been proposed.

The findings of this work can provide valuable guides for decision-making on energy-efficient designs, prefabrication, or refurbishments of container buildings among the tested subtropical region or similar climate zones.

3. Methodology

As illustrated by Figure 2, the methodology adopted for this study could be mainly divided into four phases: (1) modelling and configurations; (2) future climate prediction; (3) simulation; and (4) results and analysis.

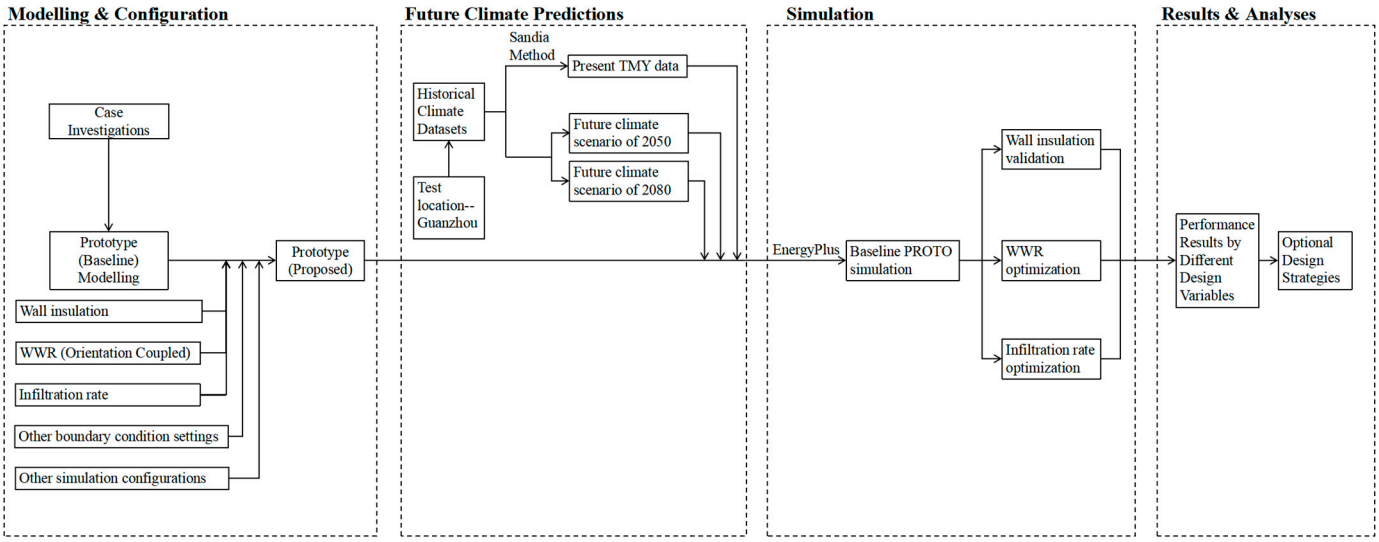

Figure 2. Flowchart of the methods used in this study.

Firstly, the baseline prototype of typical container housing was modeled based on a series of case investigations, with key design variables including window-to-wall ratio (WWR), wall insulation type, and infiltration rate, as well as other boundary conditions (envelope compositions, air conditioning schedules, etc.) and simulation settings configured.

Afterwards, historically recorded real climate datasets (2004~2018) from the International Weather for Energy Calculation (IWEC) were employed as an existing reference of meteorological data basis, while present TMY and future climate scenarios (2050 and 2080) were then both generated. The Sandia method has been used to select the present TMY data, while the future climate scenario projections have been finalized with the aid of the tool–world weather file generator under weather changes (CCWorldWeatherGen), applying the "Morphing" method and the HadCM3 climate change datasets from IPCC Data Distribution Center.

Moreover, employing OpenStudio tool (with the Energyplus engine), a series of dynamic simulation works, reflecting both energy and thermophysical performances of the modeled prototype, have been carried out to determine the key contributor of heat gains and cooling loads [29]. The energy consumption impacts of key design variables including insulation types, thicknesses, WWRs, and air infiltration rates has been validated and quantitatively revealed upon both present TMY and future climate scenarios.

Finally, based on the simulated results of energy performances, as well as comparative analyses, key conclusions have been summarized for design optimization of the container-based building typology upon future climate conditions. The most applicable envelope compositions, opening ratios, and air infiltration preferences have been proposed for future extreme climate scenarios among subtropical regions both in China and locations with similar climate conditions globally.

3.1. Test Location and Prototype Modelling

As shown in Figure 3, the selected test location, Guangzhou city, is located in the southern part of China (N 23.13°, E 113.32°). This typical subtropical climate-representative city belongs to the Hot Summer and Warm Winter zone by thermal engineering design zoning (Chinese national standard—Thermal design code for civil building GB50176-2016) [30]; therefore, it requires cooling in summer though without as much of a heating need in winter.

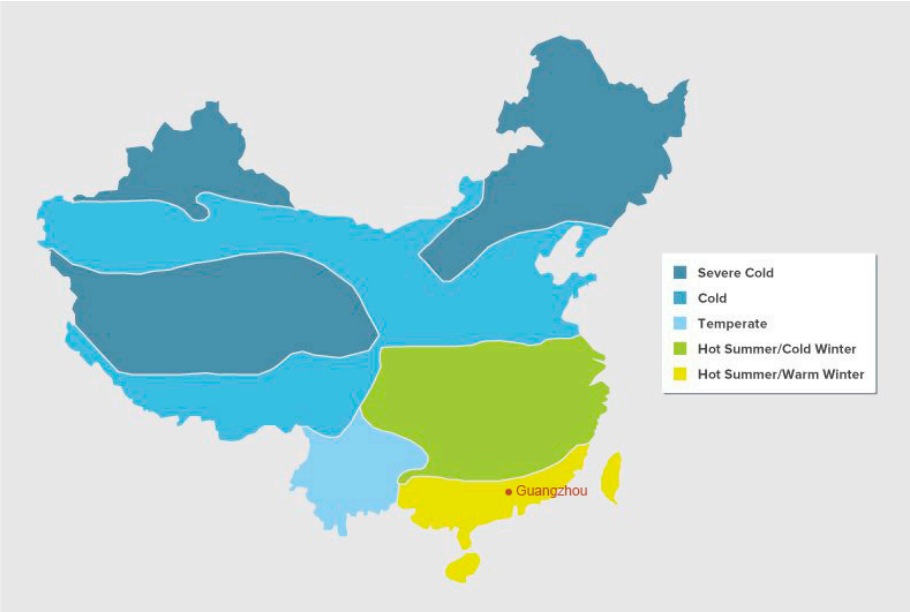

Figure 3. Location of the test city among the thermal engineering design zones of China.

Before the container housing modelling, a case investigation had been finalized. A total of 117 container project cases distributed over 20 provincial-level places in China have been studied (Figure 4), with their annual construction amount and project scale statistics shown in Figures 5 and 6.

As shown in Figures 5 and 6, the construction speed of container projects in China has remained fast-growing since 2014, and the most common form is still small-scale projects that lie in the range of 0~500 m^2. Considering the universality principle, the baseline container housing prototype was modeled by assembling four standard 40 t containers (Figure 7).

The overall building size is 12 × 4.8 × 5.8 m (length * width * height), with a total land area of 57.6 m^2 and a total building area of 115.2 m^2 over two floors. The model layouts are as shown in Figure 8.

Figure 4. Distribution of investigated container project cases around China.

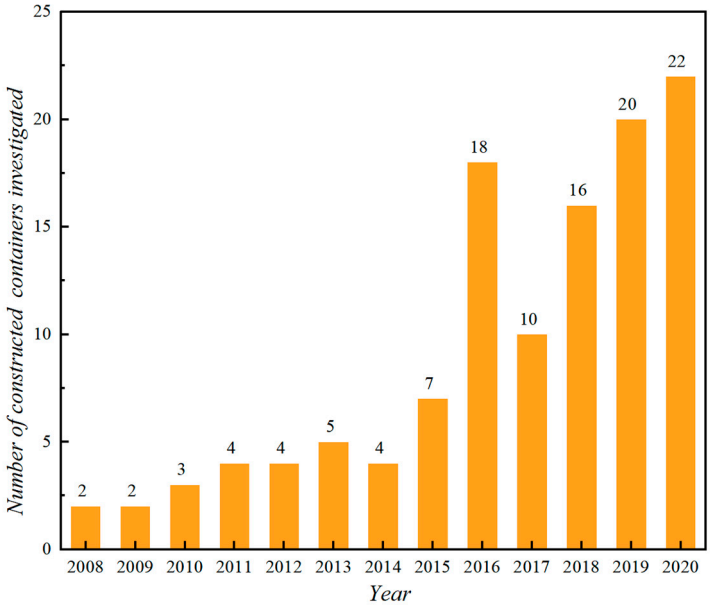

Figure 5. Annual construction statistics of investigated container project cases around China.

3.2. Envelope Configurations for Baseline Prototype

The envelope composition of the container housing baseline prototype is basically designed in accordance with the "Design Standard for Energy Efficiency of Residential Buildings in Hot Summer and Warm Winter Zone" (JGJ 75-2012) and "Technical Specification for Modular Freight Container Building" (CECS334:2013) [31,32], which comfortably meets the thermal design requirements of local residential buildings. Rigid polyurethane foam (PU) has been employed as a external thermal insulation material to ensure adequate internal space of the container. The composition details and configurations of the envelope and partitions were set as follows (Table 1).

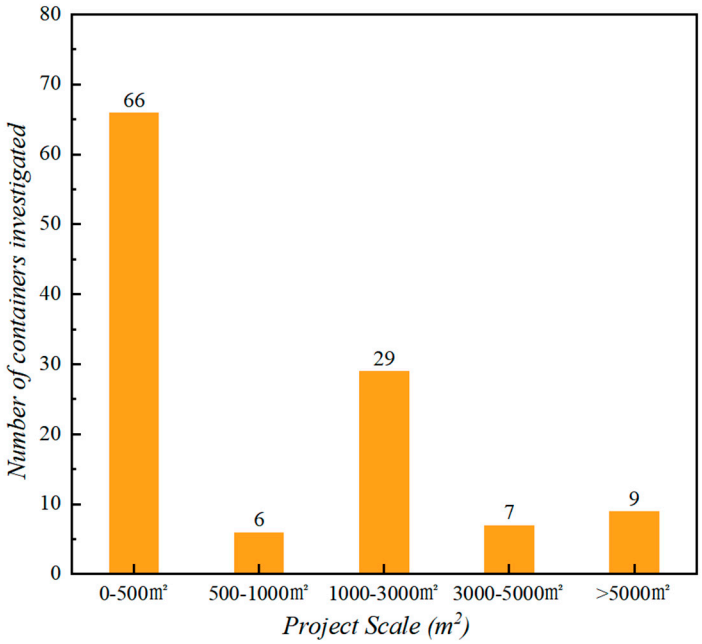

Figure 6. Project scale statistics of investigated container project cases around China.

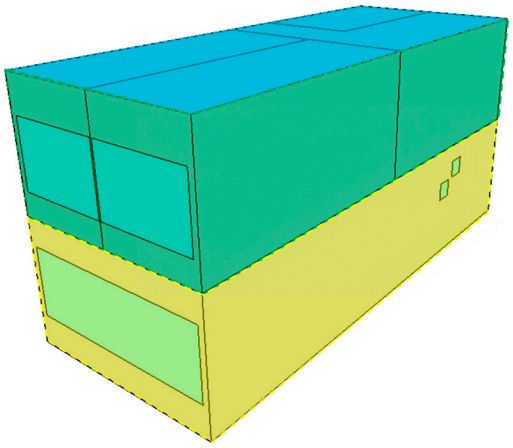

Figure 7. Modeled prototype of the container housing.

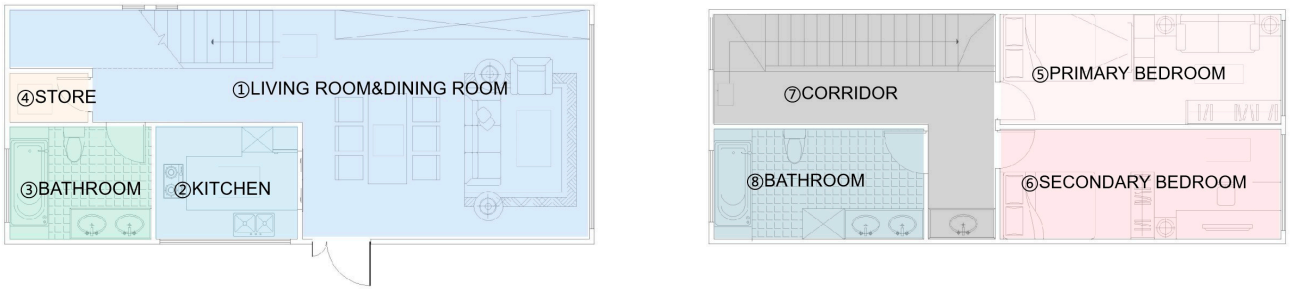

(**a**) (**b**)

Figure 8. Layout of the modeled container housing prototype for (**a**) 1st floor; (**b**) 2nd floor.

Table 1. Composition details of the container housing prototype (adapted from [31,32]).

Composition		Thermal Conductivity (W/m·k)	Specific Heat (J/kg·k)	Density (kg/m^3)	Thickness (m)
Roof	Steel plate	44.737	460	7850	0.005
	Air gap	0.188	1000	1.293	0.025
	Rigid polyurethane foam	0.026	1590	35	0.07
	Lightweight protective coating	0.29	1000	1250	0.005
	Stainless steel plate	16	480	8000	0.002
	Chipboard	0.232	1460	1000	0.01
	Gypsum board	0.407	480	1100	0.01
External Wall	Lightweight protective coating	0.29	1000	1250	0.005
	Stainless steel plate	16	480	8000	0.002
	Rigid polyurethane foam	0.026	1590	35	0.06
	Chipboard	0.232	1460	1000	0.01
	Gypsum board	0.407	480	1100	0.01
Ground Floor	Lightweight protective coating	0.29	1000	1250	0.005
	Stainless steel plate	16	480	8000	0.002
	Rigid polyurethane foam	0.026	1590	35	0.06
	Chipboard	0.232	1460	1000	0.01
	Gypsum board	0.139	5500	627	0.01
Partition walls	Cement mortar	0.29	1000	1250	0.005
	Gypsum board	0.407	480	1100	0.01

The corresponding heat transfer coefficients for the entire container housing prototype are therefore summarized below (Table 2).

Table 2. Heat transfer coefficients of the container housing prototype.

Envelope Positions	Roof	External Wall	Ground Floor	Internal Wall
Heat Transfer Coefficient (W/m^2·k)	0.344	0.418	0.410	16.95

Similarly, regarding the translucent parts of the prototype envelope, and in reference to the "Design Standard for Energy Efficiency of Residential Buildings in Hot Summer and Warm Winter Zone" (JGJ 75-2012) and "Technical Specification for Modular Freight Container Building" (CECS334:2013) [31,32], while also considering the typical opening ways employed by common container housings, configurations of windows in all orientations are specified in Table 3.

Table 3. External Window Construction details and WWRs (adapted from [31,32]).

Orientation	Material	Area (m^2)	WWR	Heat Transfer Coefficient ($W/m^2 \cdot k$)
Southern	Aluminium-plastic window with built-in blinds and sunshade transparent glass (6 mm)	15.24	0.54	2.6
Northern	Aluminium-plastic window with built-in blinds and sunshade transparent glass (6 mm)	4.88	0.18	2.6
Eastern	Aluminium-plastic window with built-in blinds and sunshade transparent glass (6 mm)	0.4	0.006	2.6
Western	Aluminium-plastic window with built-in blinds and sunshade transparent glass (6 mm)	3.48	0.05	2.6

3.3. Other Boundary Condition Settings for Baseline Prototype

Regarding the HVAC configurations, firstly, no heating is considered in subtropical regions and currently, with such small-scale container housing, no mechanical ventilation system is commonly installed; therefore, only air conditioning devices need to be configured.

As the "Design Standard for Energy Efficiency of Residential Buildings in Hot Summer and Warm Winter Zone" (JGJ 75-2012) did not regulate, both the air conditioning schedule and set point configuration followed the "Standard for Green Performance Calculation of Civil Buildings" (JGJ 449-2018), which indicated the on/off principle of split air conditioner commonly employed: "on when occupancy $\neq 0$; off when occupancy = 0" [33].

To determine the occupancy rate, relevant Chinese specifications commonly express room occupancy rates in percentages.

However, according to the above method of air conditioner schedule configuration, since almost all rooms do not have any time periods with occupancy = 0, this setting method will always keep the air conditioners in most rooms on, which obviously does not conform to the use habits of Chinese residents operating split air conditioners. Therefore, this study uses a typical Chinese household work-and-rest schedule based on investigations to set the occupancy rate of each room so as to reasonably control the air conditioning working status of each room.

According to the same standard, when the air conditioner is on, the set-point temperature is commonly configured to be 26 °C for cooling season [33]. The configuration details can be referred to Table 4.

Configuration details of other boundary conditions are summarized in Table 5. The lighting and equipment power density were configured in reference to the "Standard for Green Performance Calculation of Civil Buildings" (JGJ 449-2018) [33], and the infiltration rate was set according to the "Design Standard for Energy Efficiency of Residential Buildings in Hot Summer and Warm Winter Zone" (JGJ 75-2012) [31].

Table 4. HVAC Schedule, Set Point Temperatures and Full Occupancy Rates Configurations throughout the testing year (adapted from [33]).

	Time (Cooling Season)	**Full Occupancy Rate (Workdays: Mon–Fri)**	**Set Point Temperature (Workdays: Mon–Fri) (°C)**	**Full Occupancy Rate (Weekends: Sat–Sun)**	**Set Point Temperature (Weekends: Sat–Sun) (°C)**
1st Floor	0:00~7:30	0	/	0	/
	7:30~9:30	1	26	1	26
	9:30~18:30	0	/	1	26
	18:30~21:00	1	26	1	26
	21:00~24:00	0	/	0	/
	Time (Other Period)	**Full Occupancy Rate (Workdays: Mon–Fri)**	**Set Point Temperature (Workdays: Mon–Fri) (°C)**	**Full Occupancy Rate (Weekends: Sat–Sun)**	**Set Point Temperature (Weekends: Sat–Sun) (°C)**
	0:00~7:30	0	/	0	/
	7:30~9:30	1	/	1	/
	9:30~18:30	0	/	1	/
	18:30~21:00	1	/	1	/
	21:00~24:00	0	/	0	/
	Time (Cooling Season)	**Full Occupancy Rate (Workdays: Mon–Fri)**	**Set Point Temperature (Workdays: Mon–Fri) (°C)**	**Full Occupancy Rate (Weekends: Sat–Sun)**	**Set Point Temperature (Weekends: Sat–Sun) (°C)**
2nd Floor	0:00~7:30	1	26	1	26
	7:30~21:00	0	/	0	/
	21:00~24:00	1	26	1	26
	Time (Other Period)	**Full Occupancy Rate (Workdays: Mon–Fri)**	**Set Point Temperature (Workdays: Mon–Fri) (°C)**	**Full Occupancy Rate (Weekends: Sat–Sun)**	**Set Point Temperature (Weekends: Sat–Sun) (°C)**
	0:00~7:30	1	/	1	/
	7:30~21:00	0	/	0	/
	21:00~24:00	1	/	1	/

Table 5. Configuration details of other boundary conditions (adapted from [31,33]).

Room Number	**Area (m^2)**	**Lighting Power Density (W/m^2)**	**Equipment Power Density (W/m^2)**	**Infiltration Rate (ACH)**
1	41.16	6	6	1
2	7.2	6	6	1
3	7.2	6	4	1
4	2.04	5	0	0
5	14.4	5	6	1
6	14.4	5	6	1
7	18	5	4	1
8	10.8	6	4	1

3.4. Key Design Variables

Considering that the main energy-saving demand of the test area is anti-heat gains, and in reference to the energy-saving design focus of general residential buildings by the relevant standard [31], this study selects the WWR, opaque wall insulation, and air infiltration rate as the key optimization design variables. Their variation impacts over the container cooling energy consumption were then investigated throughout the validations by means of dynamic simulations. The variable range of all the parameters has been summarized in Table 6.

Table 6. Key design variable ranges.

Variable Name	Variable Range
insulation material type	polystyrene foam board, rigid polyurethane foam, rock wool board, mineral wool board, cement expanded perlite, cement expanded vermiculite
insulation layer thickness	50~100 (mm)
WWR	0.2~0.4
air infiltration rate	0.5~1.5 (ACH)

Only external insulation has been considered, as internal insulation is commonly not preferred by Chinese residents due to unwanted area losses. VIP is still not well-applied due to relatively high costs. In reference to the Chinese "Technical standard for external thermal insulation on walls" (JGJ 144-2019) [34], six insulation materials in three types, which are all affordable and widely used in China among ordinary low-rise and multi-story buildings, had been selected as insulation material choices.

The insulation layer thickness range was also determined in reference to the same standard [34] and considering the conventional value range as well as product specifications; as in most cases, the insulation starts from 50 mm while not exceeding 100 mm in China.

The variable range of WWR has been determined in reference to the "Design Standard for Energy Efficiency of Residential Buildings in Hot Summer and Warm Winter Zone JGJ 75-2012" [31]. Unlike in northern China, in the Hot Summer and Warm Winter Zone, WWR is recommended with limited value to balance between the daylighting and anti-heat gains, so 0.2~0.4 has been ranged.

The air infiltration rate values have also been ranged in reference to the same standard [31] and relevant local infiltration rate research [35]. It seems that 0.8~1.0 (ACH) is the higher probable range, but a range of 0.5~1.5 (ACH) is worth investigation.

For different insulation material types, the detailed thermal physical properties have also been given in Table 7.

Table 7. Thermal physical properties of different insulation materials studied.

Insulation Material Types	Insulation Material Names	Density (kg/m^2)	Thermal Conductivity (W/m·k)	Heat Storage Coefficient ($W/m^2 \cdot k$)	Specific Heat Capacity (J/kg·k)
Plastic type	polystyrene foam board	42	0.0247	0.33	1500
	rigid polyurethane foam	35	0.026	0.36	1590
Rock wool type	rock wool board	95	0.045	1.22	750
	mineral wool board	187	0.042	1.34	750
Vermiculite type	cement expanded perlite	400	0.16	2.49	1170
	cement expanded vermiculite	350	0.14	1.99	1050

3.5. Climate Data

This work refers to the IWEC datasets as the historical meteorological data (2004~2018) to be taken as the Reference Year (RY) for the present TMY and future climate scenario data forecasting.

For the future scenario prediction and considering climate change, this study was based on the more widely used global regional climate model with the more accurate spatial resolution. It applies the Morphing downscaling method developed by Belcher, Hacker, and Powell [19,36–40], which maintains the existing climate's features while integrating expected climate changes for the set time points to generate new meteorological scenario datasets. Based on the high uncertainty of future climate change, in this work, the IPCC climate prediction scenarios covering the various possibilities of future development are mainly employed for future climate predictions. Considering all climate scenarios of SA90, IS92, SERS, and RCPs successively released in previous IPCC reports, the most widely used SERS prediction scenario at present was selected for this study. It envisages four different social development scenario groups (A1, A2, B1, B2) induced by varied impacting factors, exhibiting little difference at first but can result in extraordinary disparities by 2100 [41]. The greenhouse emission occasions of the four groups implying six different development scenarios. Among them, considering the current social and economic development and population growth, the future climate change is selected from the A2 prediction group and adapts currently widely used SERS scenarios published in the previous IPCC assessment reports. It corresponds to a future development occasion in which the population continues to grow, but the fertility rate increases slowly. A medium-to-high-speed growth model and social development scenario still maintains rapid economic growth and increased carbon emissions.

Among various climate factors affecting building energy consumption, dry bulb temperature, solar radiation, and moisture content are studied by the Morphing method, while relative humidity is obtained through the prediction of related climate parameters, with wind speed remaining unchanged. Dry bulb temperature, solar radiation, and moisture content shall be calculated as follows:

$$T = T_0 + \Delta T_m + (T_0 - \langle T_0 \rangle_m) \tag{1}$$

$$\alpha_{T_m} = \frac{\Delta T_{MAX,m} - \Delta T_{MIN,m}}{\langle T_{0max} \rangle_m - \langle T_{0min} \rangle_m} \tag{2}$$

where T, T_0—hourly dry bulb temperature in the future and present, °C; $\langle T_0 \rangle_m$, $\langle T_{0max} \rangle_m$, $\langle T_{0min} \rangle_m$—monthly average dry bulb temperature, daily maximum and minimum dry bulb temperature, °C; ΔT_m, $\Delta T_{MAX,\,m}$, $\Delta T_{MIN,\,m}$—monthly average dry bulb temperature change, daily maximum and minimum dry bulb temperature, °C; α_{Tm}—scaling expansion coefficient of dry bulb temperature drop;

$$\alpha_{H_m} = 1 + \frac{H_m}{100} \tag{3}$$

$$H_R = H_{R0} \times \alpha_{H_m} \tag{4}$$

where H_R, H_{R0}, H_m—predicted hourly change percentage of relative humidity and monthly change percentage of moisture content in the future and present; α_{Hm}—scaling expansion coefficient of moisture content;

$$\alpha_{R_m} = 1 + \frac{\Delta R_m}{I_{0m}} \tag{5}$$

$$I = I_0 \times \alpha_{R_m} \tag{6}$$

where I, I_0, I_{0m}—hourly solar radiation in the future and present, as well as monthly mean value of current solar radiation, W/m^2; ΔR_m—monthly predicted value of horizontal solar radiation change; α_{Rm}—scaling expansion coefficient of solar radiation.

Through adopting the CCWorldWeatherGen developed by the Sustainable Energy Research Group at the University of Southampton, UK [42], the corresponding meteorological data under the SERS-A2 emission scenario [41] could be predicted and generated based on the "Morphing" method combined with the HadCM3 model [43]. According to the HadCM3 climate change datasets provided by the IPCC Data Distribution Center [41], the monthly values describing the relative climate changes in between the historical data during the years 1961–1990 and the future data of the years 2050 and 2080 were loaded into CCWorldWeatherGen. Afterwards, the historical climate datasets of Guangzhou (2004–2018) were obtained from the climate database Climate One Building, and the present TMY climate data were determined adopting the widely applied Sandia method. The relative changes of meteorological data, as well as future novel meteorological data, can be obtained by loading the new TMY climate file into CCWorldWeatherGen. Two future periods in the 2050s (2041–2070) and 2080s (2071–2100) have been considered separately to examine the future climate scenarios.

3.6. Simulation Tools

To finalize the dynamic energy simulations, the Energyplus calculation engine together with OpenStudio interface has been chosen.

Firstly, in order to accurately reflect the impact of design variables on the overall energy performance of the whole building, it is necessary to have a calculation platform that has been widely validated for the reliability of its calculation results. As one of the few whole-building energy modeling engines, Energyplus has been used for more than 20 years and has been widely employed for all kinds of building simulation tasks [44]. The accuracy of its simulation results have been universally verified.

Secondly, because this research focuses on the optimization of the building envelope rather than the HVAC system, the Energyplus platform, which is more convenient for the detailed setting of the building body itself (e.g., the variable setting of the building envelope) is more applicable than other tools that are good at system simulation (e.g., TRYSYS).

Finally, although the prototype modelling of this study is not so complex and there are no parametric design needs, it is not necessary to use a powerful parametric modelling interface such as Grasshopper+Honeybee. However, in order to reduce the difficulty of prototype modeling and adjusting over the Energyplus platform, a user-friendly interface tool is still needed for efficiency. Therefore, OpenStudio is finally selected as the interface tool to match the Energyplus simulation engine for this research.

4. Results

4.1. Upcoming Climate Prediction

Figure 9 shows the predicted monthly average dry bulb temperatures of key future climate scenarios (2050 and 2080). It can be seen that for both scenarios, monthly average dry bulb temperatures meet clear increments, and the increments in the winter period are larger than that in the summer period. It also reflects the obvious trend towards more extreme climate conditions in the future.

Figure 10 illustrates the predicted monthly average relative humidities of the same future climate scenarios (2050 and 2080). Contrary to the dry bulb temperature, future relative humidities exhibit decrements comparing to present values in overall, especially during the summer period, while in the winter period the decrements appear to be relatively smaller. Considering the higher temperature coupled with less latent heat thanks to the lower air moisture, the summer cooling loads of the future scenarios tend to be too complicated to maintain the indoor comforts of container housings.

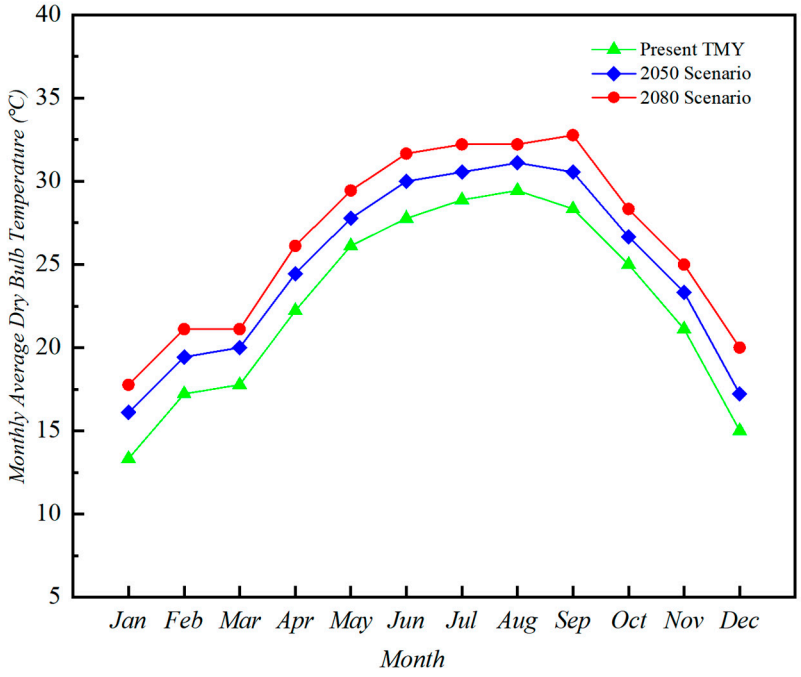

Figure 9. Monthly average dry bulb temperatures of present TMY and predicted future scenarios (2050 and 2080).

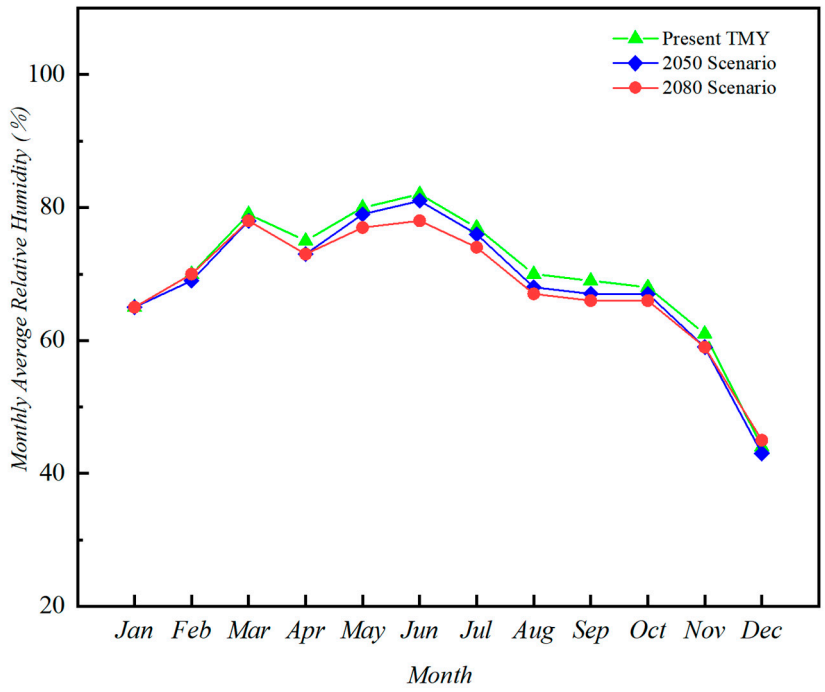

Figure 10. Monthly average relative humidities of present TMY and predicted future scenarios (2050 and 2080).

The predicted total monthly solar radiations are shown by Figure 11. It can be seen that during the spring and autumn, the total monthly radiation meets no big change in the near future. During the summer period, the total month radiation slightly decreases, and during the winter period it shows modest increases when compared to present conditions.

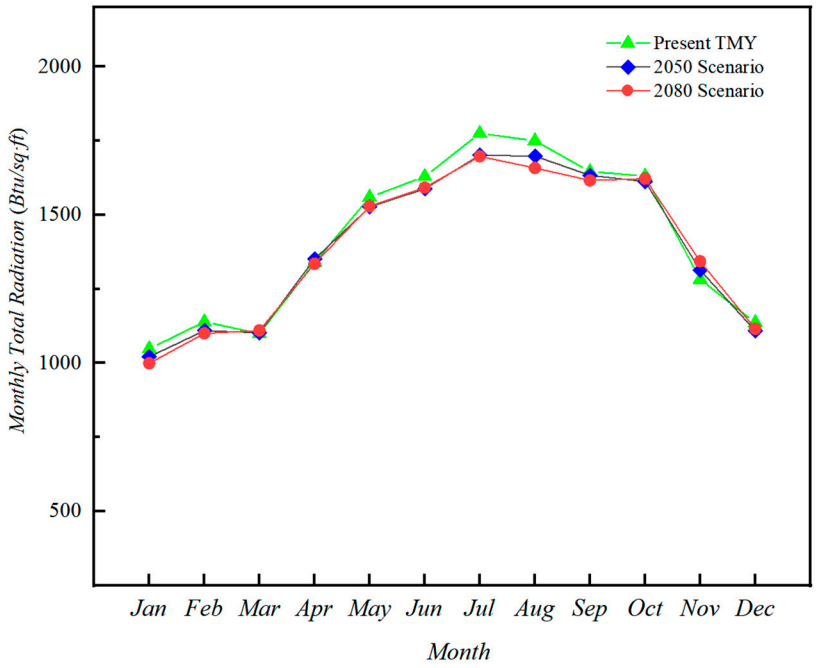

Figure 11. Total monthly radiations of present TMY and predicted future scenarios (2050 and 2080).

4.2. Thermophysical Behaviour of Typical Cooling Season Day

A typical summer day (21st July) was chosen to demonstrate the thermophysical behavior of the container housing prototype during the cooling season. It can be seen from Figure 12 that all four data series have slight increments. For present TMY climate data, the maximum outdoor temperature of the summer testing day reached 35 °C at 14:00 p.m., while for the 2080 scenario it also reached the upper limit at 14:00 p.m. but was 0.9 °C higher to arrive at 35.9 °C. Regarding the temperature of the external top surface, a similar phenomenon has been observed. Due to continuous direct radiations, the temperature of the container top surface can be much higher than the air temperature in summer. For both the present and 2080 scenarios, the maximum temperatures on the top external surface of the container prototype appeared at 12:00 noon, equaling to 73.59 °C and 74.04 °C, respectively, with little difference.

The container indoor temperatures change with the intermittent operation of the air conditioner. When the air conditioner was working, the indoor temperatures kept stable at the set point level, while when it was not working, the indoor temperatures fluctuated with the outdoor temperatures. The results show that regardless of the current or future scenario, container indoor temperatures kept constant at 26 °C during refrigeration periods, while after the air conditioner was switched off the indoor temperatures both reached the peak at around 16:00 p.m. For the present and 2080 scenarios, the predicted indoor temperatures arrived at 35.65 °C and 36.18 °C, respectively, with only a 0.53 °C difference.

Regarding the cooling energy consumption, the performance due to the present climate is generally similar to that due the future scenario, while the energy level of the latter is only slightly higher than that of the former. For both occasions, the cooling consumption is equal to zero when the air conditioner is off. However, when it is on, both scenarios met the load peaks at around 9:00 a.m. and 18:00 p.m., and both reached the maximum value at around 18:00 p.m. The peak values of present and future scenarios are 20 MJ and 21 MJ, respectively, with a minor improvement of 1 MJ. For both scenarios, the energy peak occurred when the temperature difference between indoor and outdoor were maximum. This implies the fact that, even upon more extreme climate conditions in future, the cooling load variations are closely related to the indoor and outdoor temperature disparities.

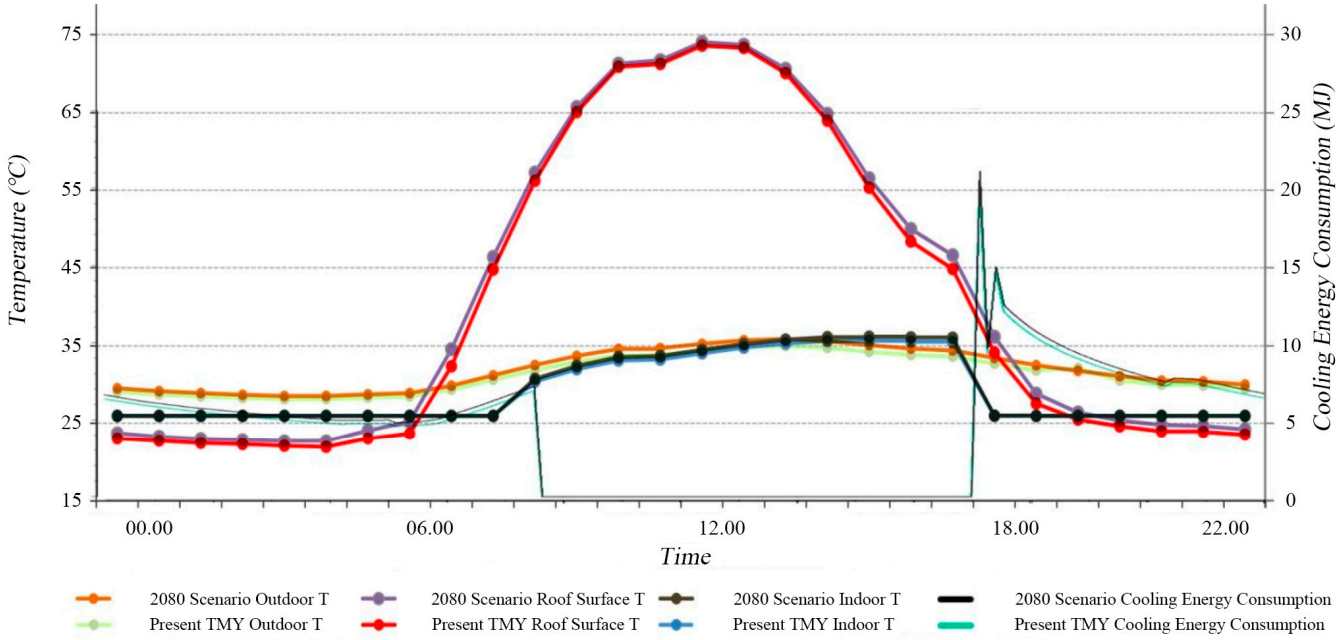

Figure 12. Thermal–physical behaviors of container housing prototype for present TMY and predicted 2080 scenario.

4.3. Performance of Baseline Prototype

4.3.1. Thermal Performance

It can be seen from Figure 13 that, upon the future outdoor temperature elevation predictions based on the present TMY conditions, the indoor temperature of container buildings will also increase clearly throughout the cooling season (April–September), even if air conditioners are employed. In addition, through the transition seasons except April to September, and especially during October to November when the indoor temperature is not regulated by the air conditioner, even more obvious increases can be observed. In winter, facing the future outdoor temperature rise, there are less risks of a low temperature period and the need for heating among this climate area.

For both phenomena, the long-term period's (2050–2080) growth is always more obvious than the recent period's (present–2050) growth.

4.3.2. Energy Performance

In order to better reflect the energy efficiency disparities upon future climate scenarios in both near- and long-terms, the difference in energy consumption levels in between the present TMY, 2050, and 2080 scenarios has been further studied. Based on the consumption statistics for the complete cooling season (Figure 14), it can be seen that by passing from present TMY to the 2050 scenario, the total cooling demand of the prototype increased by 16.4%, while from predicted 2050 to 2080 scenarios it increased by 13.3%. More specifically, both envelope heat gains and infiltration experienced clear increments, while internal heat gains mainly composed of equipment and people remained almost unchanged throughout the time slot. This fact implies that the outdoor temperature increase shall dominate the energy consumption growth in the face of future extreme climates. In addition, for both occasions envelope heat gains attained around more than half of the cooling loads, while infiltration amounted to around one-fourth.

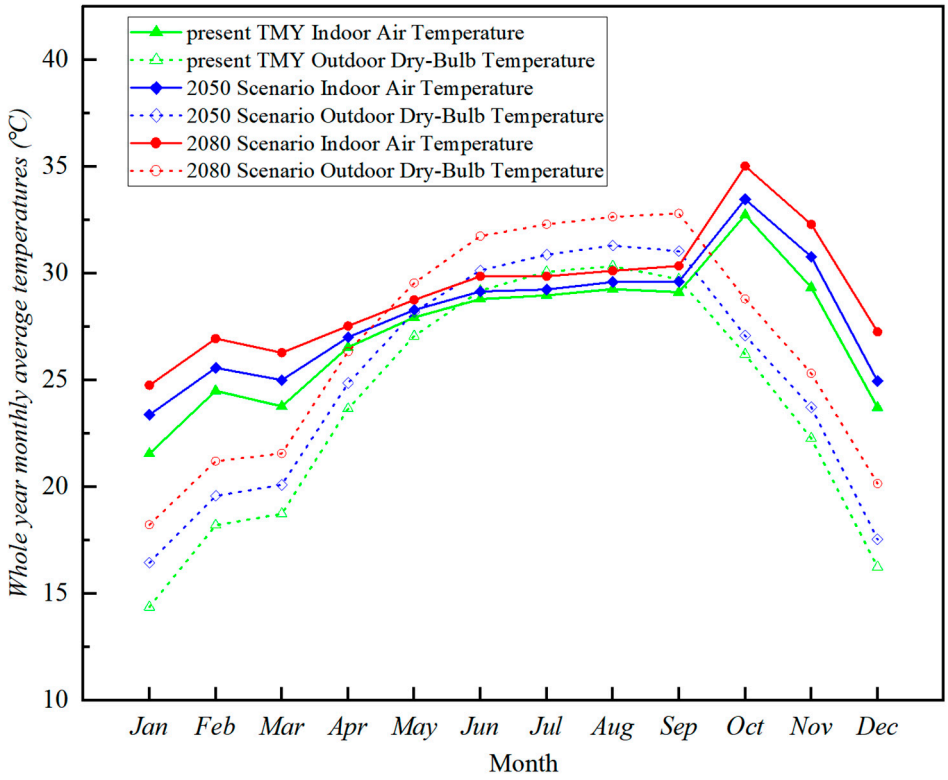

Figure 13. Whole year monthly average temperatures of present TMY and predicted future scenarios (2050 and 2080).

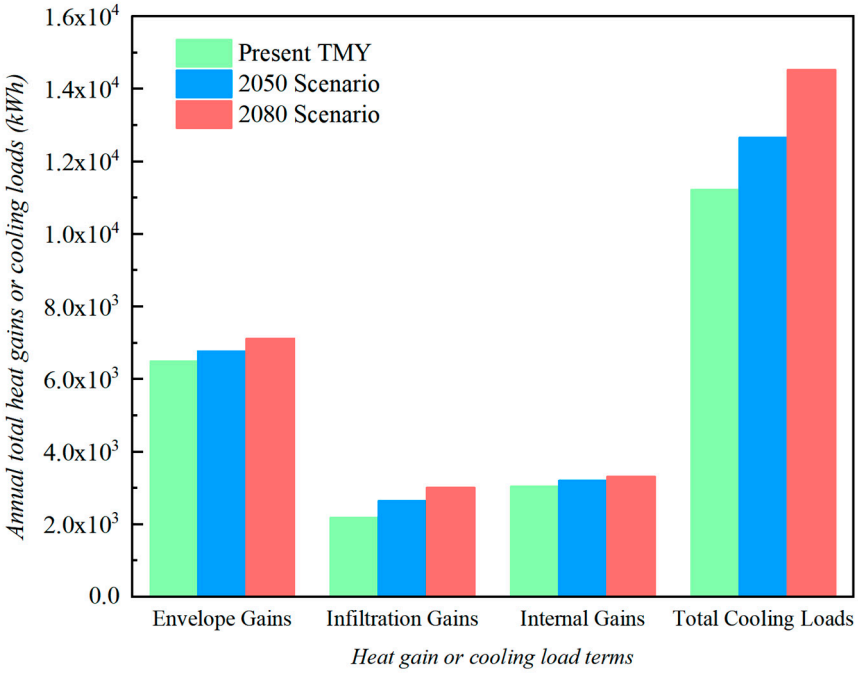

Figure 14. Heat gain terms of the total cooling loads of present TMY and predicted future scenarios (2050 and 2080).

4.4. Envelope Optimizations

Based on above obtained discoveries, further analyses were carried out in order to evaluate the actual impacts that envelope properties may have on container cooling energy demands, based upon the critical climate scenarios of 2050 and 2080.

4.4.1. Opaque External Wall Composition

Firstly, the possibilities of reducing the cooling demands by alternating the external wall compositions (insulation materials and thicknesses) were examined. Simulation works were conducted for the present TMY and future climate scenarios of year 2050 and 2080. The results in Figure 15 show that for all test time occasions, among all types of insulation materials examined with same thicknesses, plastic type, and rock wool type, thermal insulations (polystyrene foam board, rigid polyurethane foam, rock wool, and mineral wool) can provide the relative best thermal performances, while the vermiculite type (cement-expanded perlite and cement-expanded vermiculite) exhibits worse insulation performances. The performances of different insulation materials follow the sequence of polystyrene foam board > rigid polyurethane foam > rock wool > mineral wool > cement expanded vermiculite > cement expanded perlite. The heat transfer coefficient of the vermiculite type with the same thickness is more than twice that of the rock wool type once, and more than four times that of the plastic type. This has also caused huge differences in annual cooling loads. Vermiculite-type insulation boards of the same thickness can often cause a cooling load almost twice the level of the plastic-type insulations.

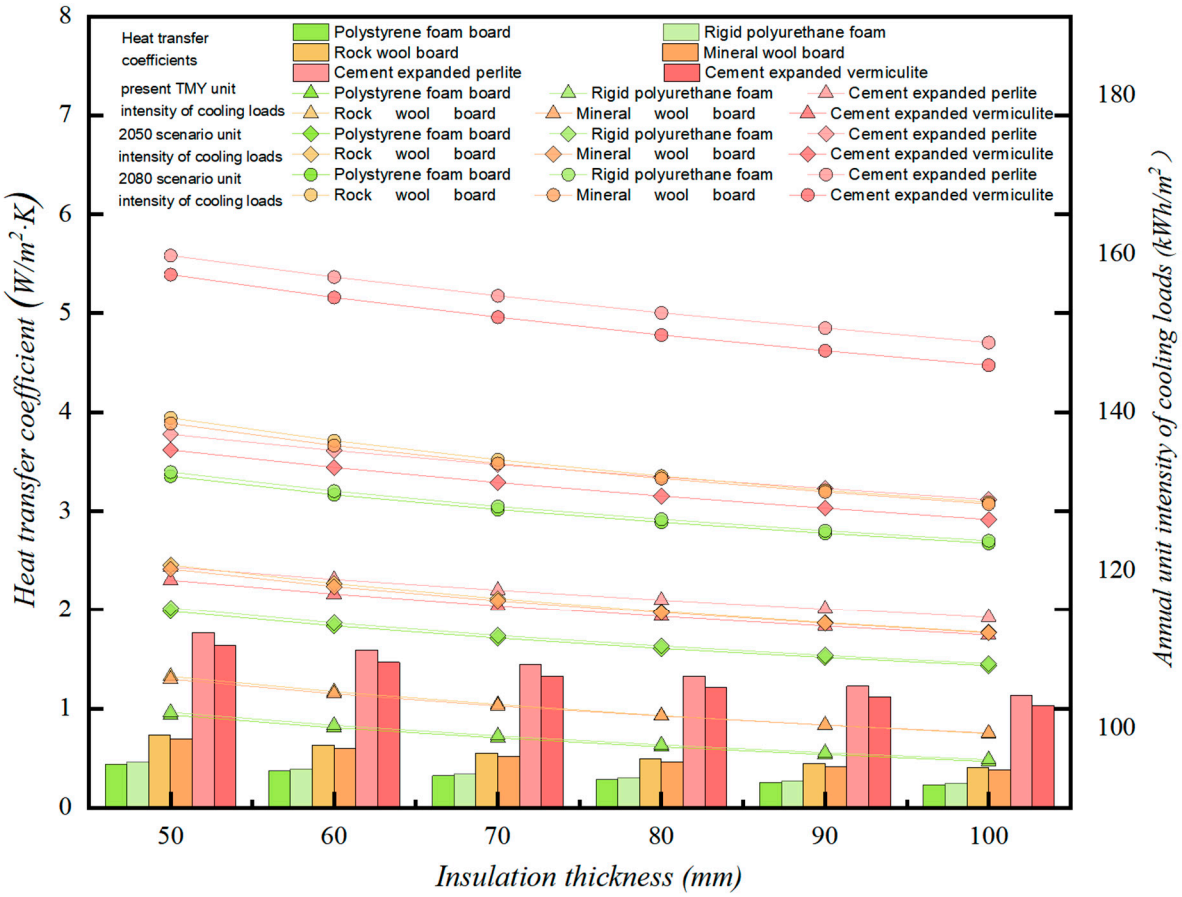

Figure 15. Annual unit intensity of cooling loads due to various wall insulation materials and thicknesses of present TMY and predicted future scenarios (2050 and 2080).

Regarding the suitable thicknesses of all insulation types, and in reference to the actual energy reduction performances, the best thickness of plastic insulation materials should be set in the range of 70~90 mm, while the expanded perlite and vermiculite types do not reach satisfactory thermal performance even with a thickness larger than 100 mm; therefore, they are not suggested. Among different types of plastics, polystyrene foam board and rigid polyurethane foam maintain a suitable thickness in the range of 70~80 mm, while rock wool and mineral wool are suggested with a thickness in the range of 80~90 mm. The critical

meaning of these suggested thickness thresholds lies in the fact that with thicknesses below these thresholds, effective energy consumption reduction can be observed with thicker insulations, while when the thicknesses exceed them the energy consumption becomes almost unchanged.

For both present and future TMYs, there are no significant differences seen for the above results. With future scenarios, the main load differences due to insulation variations lie in the fact that when same type and same thickness of thermal insulation get employed, the annual cooling load unit intensity in the 2080 scenario is significantly higher than that of the 2050 scenario—which is also significantly higher than that of the present TMY conditions.

4.4.2. External Wall WWR

Secondly, WWR could be another important design factor of envelope optimizations. Increasing WWR means better indoor daylighting and exterior view, but also apparent increases of heat gains which can lead to abundant cooling loads. Considering the comparatively much larger heat transfer coefficient of windows than opaque walls, the selection of reasonable WWRs is surely a critical factor for the energy efficiency of container buildings. Thus, corresponding simulations in various orientation-coupled external WWRs upon the future climate scenarios (2050 and 2080) had been carried out accordingly.

Figure 16 shows that for all orientations smaller WWRs can lead to reduced cooling loads. Eastern and western façades are more sensible to WWR variations in comparison to southern and northern ones, and even a small WWR in the east or west side will bring a large amount of extra cooling load, implying that special attention should be paid to the eastern and western façade designs. On the contrary, for southern and northern façades, WWRs exhibit relatively less impact and therefore there can be more freedom for designs. Meanwhile, due to living needs, too small a WWR should also be avoided, and moderate values could be the best choices.

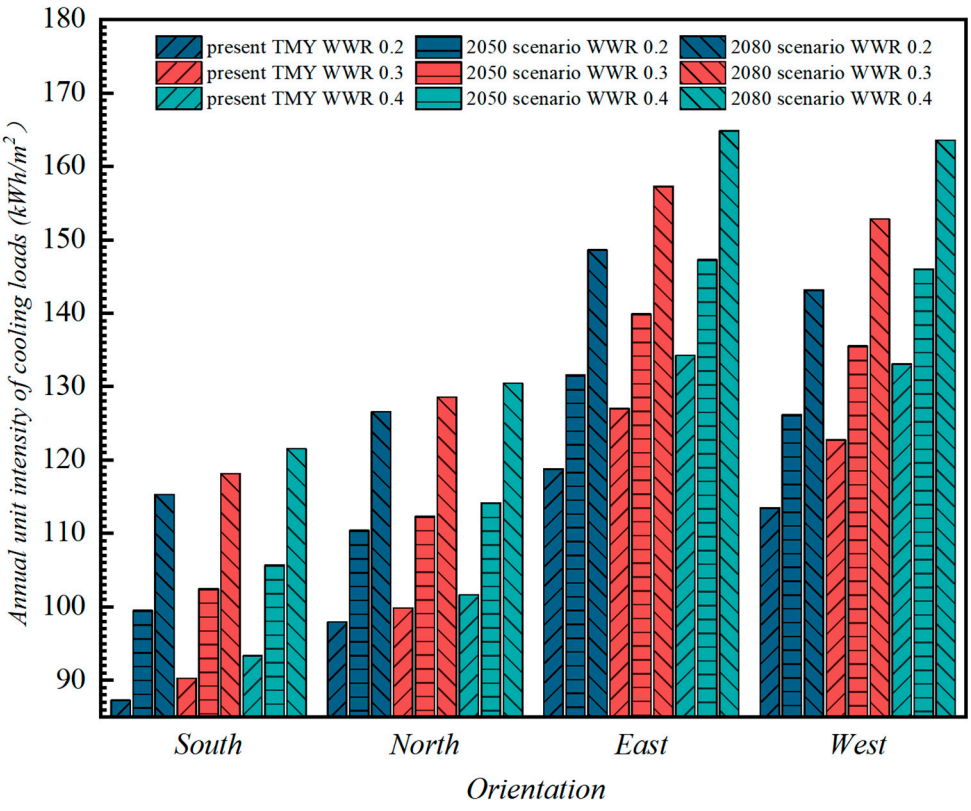

Figure 16. Annual unit intensity of cooling loads due to various wall orientations coupled WWRs of present TMY and predicted future scenarios (2050 and 2080).

4.4.3. External Wall Infiltration

Finally, considering that infiltration heat gains account for around one-fourth of the total cooling demand in container housings (Figure 17), the sensitivity of the annual unit cooling load intensity and annual unit infiltration heat gains towards infiltration rates was also further analyzed. Based on one time air change per hour (ACH = 1) as the baseline level of the infiltration rate, the ACH range of 0.5~1.5 has been surveyed. It can be seen from Figure 15 that, with the increase of the air exchange rate, heat gains through the envelope due to infiltration shows a steady upward trend. The unit cooling load intensity also maintains an ascending trend, which is in general larger than the infiltration heat gains. However, the ascending rate tends to slow down with higher ACHs. These results can obviously indicate that higher infiltration can contribute significantly to higher infiltration heat gains and, therefore, higher cooling load intensities. This trend is very similarly seen in the present TMY, 2050, and 2080 scenarios. The only difference is that when compared to the present TMY, the infiltration heat gains and unit cooling load intensities in 2050 and 2080 are both clearly higher (15% higher for infiltration heat gains and 22% higher for unit cooling load intensity in 2050 than present; 13% and 20% higher for 2080 than 2050). This implies the fact that the cooling energy burden brought by infiltration would be further highlighted upon more extreme future climate conditions. Therefore, compared with the baseline prototype level, a stricter infiltration rate should be controlled to cope with future extreme climate conditions.

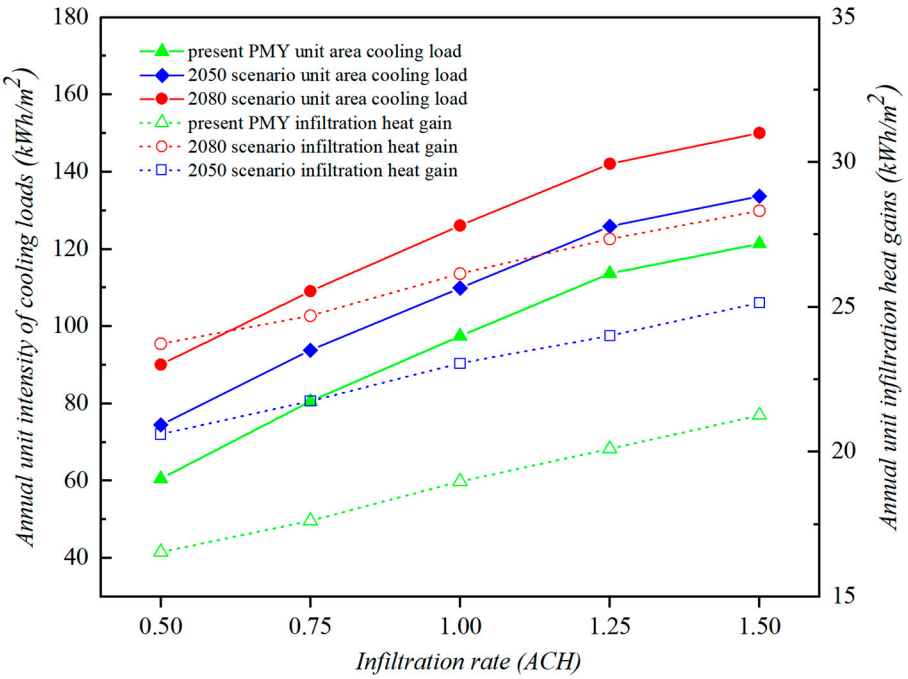

Figure 17. Annual unit intensity of cooling loads and unit infiltration heat gains due to various infiltration rates of present TMY and predicted future scenarios (2050 and 2080).

4.4.4. Beneficial Effects of Coupled Envelope Optimizations

On the basis of above independent optimization validations of each variable and in order to explore the coupled energy-saving benefits through simultaneous application of all design variables, the baseline prototype has been concurrently optimized for the insulation materials, WWRs, and infiltration rates of its envelope at the same time. The actual coupled optimization effects of all variables have then been examined through the dynamic simulations of the optimization models for their thermal environments and annual cooling loads, in both present (present TMY) and future climate scenarios (2050 and 2080 scenarios).

In order to fully reflect the optimization effects of all key design variables, on the basis of baseline model configurations, the 100 mm thick polystyrene foam board has been selected as the thermal insulation reference while 0.5 (ACH) has been set as the infiltration rate reference for all optimization models. For WWR optimizations, since different WWRs were originally configured for each facade of the baseline model, the corresponding optimization configurations become slightly complicated. For the eastern and western elevations, which are more sensitive to WWR variations, lower WWR values have been configured for the baseline model than the independent variable optimization studies. In order to avoid the simultaneous deterioration impacts of larger WWRs to go along with the coupled effect of optimized insulation materials and infiltration rates, the optimization models maintain the same WWRs of the eastern and western facades of the baseline model. In the northern and southern facades that are comparatively insensitive to WWR variations, the baseline model has employed similar or higher WWR values than the independent variable studies (0.5 for the southern and 0.18 for the northern facades). To fully reflect the optimization effect of WWRs, a uniform WWR value of 0.2 has been configured for both the northern and southern facades of all optimization models.

Based on the above configured optimization values of all variables, dynamic simulations validating the thermal environments and annual cooling loads of optimization models upon all climate scenarios have been conducted. The results show that (Figure 18) upon all scenarios (present TMY, 2050, and 2080 scenarios), the optimization models that apply coupled envelope optimization measures all met significant reductions of indoor temperatures throughout the year. Through the transition seasons without air conditioning, the indoor temperature mitigation effects brought by the coupled envelope optimization were particularly obvious. This is further evidenced by the fact that the above envelope optimization measures all maintain significant impacts on the indoor thermal comfort improvements of subtropical container buildings, and they also can achieve appreciable coupled energy-saving benefits when they are jointly implemented.

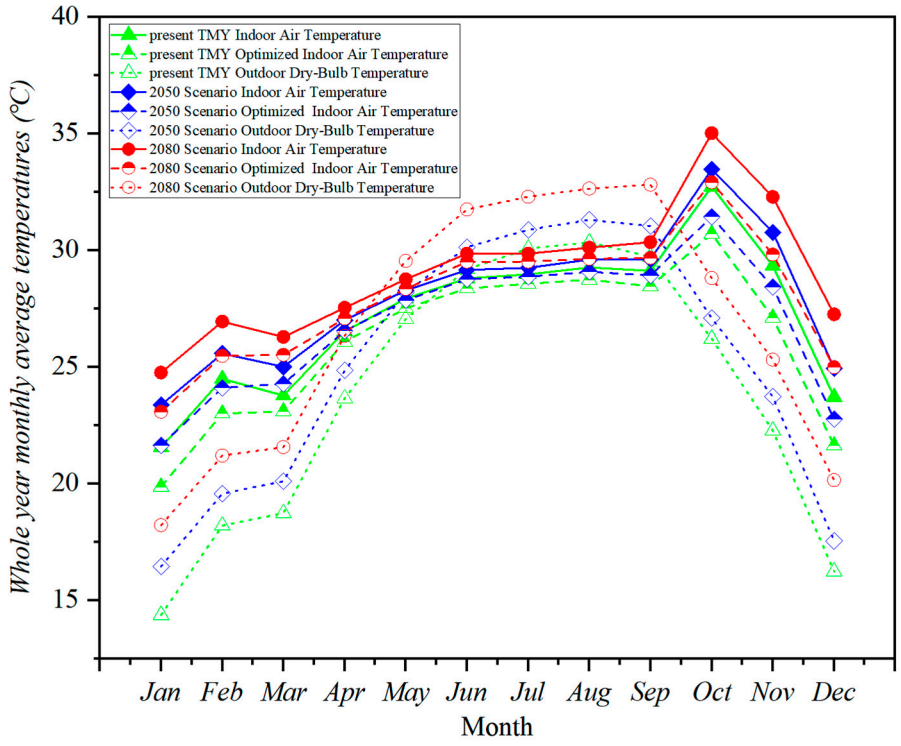

Figure 18. Whole year monthly average temperatures of baseline and optimized prototypes upon present TMY and predicted future scenarios (2050 and 2080).

Similar to the indoor thermal environment, the optimization models that simultaneously adopts all envelope optimization measures in response to various climate scenarios (present TMY, 2050, and 2080 scenarios) have also shown obvious energy-saving advantages (>10%) (Figure 19). The energy-saving benefits given by adopting coupled optimization measures when compared to the baseline references are also relatively similar in each climate scenario. The results prove once again the significant effectiveness of conventional envelope design measures for controlling the impacts on the container cooling loads, in consideration of subtropical regions in future extreme climates.

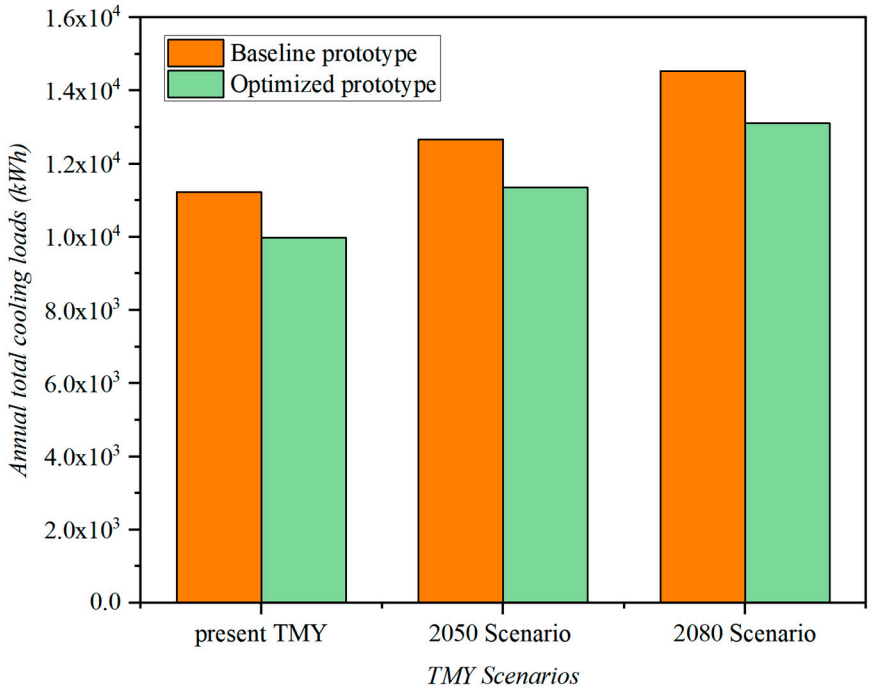

Figure 19. Annual total cooling loads of baseline and optimized prototypes upon present TMY and predicted future scenarios (2050 and 2080).

However, it can also be found that the simultaneous employment of different optimization measures cannot simply lead to the superposition of energy-saving effects by independent variable optimizations. In other words, the collaborative optimization of each design variable may weaken the energy-saving effects of the other variables. Even so, the simultaneous improvements of both the thermal performance and airtightness of container envelopes can still achieve remarkable and comprehensive energy-saving benefits.

5. Discussions

The obtained results of the baseline model performances on a typical day of extreme seasons regarding the thermal environments and cooling loads can tell us many things.

First of all, compared with the occasion under present TMY, the outdoor temperatures, roof external surface temperatures, and indoor temperatures in future climate scenarios all rise clearly, which confirms the extreme future climate expectations. It can therefore be predicted that all temperature indicators in the summer season of the subtropical region would be improved upon such future climate expectations.

Secondly, the fact that the indoor–outdoor temperature difference and the load peak both appear at the same time of the day for both the present TMY and future climate scenarios indicates that no significant difference of the daily temperature changing rule can be observed upon future climate scenarios, even though the climate conditions tend to be more extreme for the investigated climate region. The direct correlation between the indoor–outdoor temperature differences and the cooling loads is also not expected to change.

Based on the above facts, it can be inferred that upon future extreme climate scenarios, the effective optimization measures and modes of the heat proof design should not change much for container buildings in the subtropical region. Therefore, it is feasible to redevelop and employ conventional envelope design measures to reduce the impacts of future extreme climate conditions on the cooling loads and indoor thermal environments.

What follows next are the results about the annual cooling load and thermal environment of the baseline model.

Firstly, in response to the future extreme climates of the subtropical region, both the indoor temperature enhancements and the envelope heat gain increases of the container buildings exhibit close relationships with the outdoor temperature rises. With regard to indoor temperature enhancements, throughout both the refrigeration season when air conditioners are used to regulate room temperatures and the transition seasons when air conditioners are constantly off, the indoor temperatures of container buildings ascend significantly with the increased future outdoor temperatures. Regarding the annual cooling load increases, through the comparative analysis of both envelope and internal heat gains it can be concluded that the elevated envelope heat gains induced by future increased outdoor temperatures can be accounted as the main contributor of cooling load rises. Relatively speaking, the internal heat gains were almost unchanged in future climate scenarios.

Secondly, among the additional envelope heat gains induced by outdoor temperature increases of this climate zone, the heat gains because of envelope thermal transfers are almost on a par with the ones due to hot air infiltration, both acting as important contributors of the cooling load growth. It shows that outdoor air temperature rises can bring equivalent impacts on both envelope thermal transfers and the hot air infiltration, both of which will cause obvious increases in external envelope heat gains.

The new findings based on this is that the heat-proof designs in this climate zone in extreme future climates should first focus on the control of envelope heat gains caused by the outdoor temperature increases rather than the internal heat gain rises. In particular, attention should be paid to both the thermal property optimizations and infiltration level restrictions of the external envelopes.

On the basis of the above understandings and the corresponding annual cooling load simulation results of optimized prototypes in both the present TMY and future climate scenarios, the actual impacts of key variable optimizations in the subtropical climate zone follow.

Firstly, among the examined three types of economic thermal insulation materials commonly employed in Chinese dwellings, the cooling loads of prototypes adopting plastic- or rock wool-type insulation are often close to half the level of the ones adopting vermiculite-type insulation of the same thickness, which implies the huge energy-saving advantages of plastic- and rock wool-type insulation materials. When these two insulation types got selected, a medium-to-thick material thickness (70~90 mm) can already achieve satisfactory energy-saving effects for the medium-future term (2050 scenario), while for the long-future term (2080 scenario) a thick material thickness (90~100 mm) may be required to achieve similar heat-proof effects.

Secondly, for the WWR impact evaluations in different orientations, it has always been the smaller WWRs that are more conducive to the annual cooling load control. In addition, the WWR changes in the eastern and western facades clearly show higher impacts on the annual cooling loads than the changes in the northern and southern facades. Considering both the daylighting and energy-saving demands, it can be deduced from the results that upon the future extreme climates it would be even more necessary to make trade-offs between natural illumination and energy conservation for defining the window proportions. The sacrifice of eastern and western side WWRs can be regarded as more valuable and meaningful for energy savings than the expenses of northern- or southern-facade window areas.

In addition, the validation of airtightness impacts shows that the additional heat gains and cooling loads—because of the infiltration—would increase obviously in future extreme

climate conditions, even at the same infiltration rates. The steady increase of the infiltration rates can directly lead to the stable growth of the infiltration heat gains, as well as the slowing growth of the annual cooling loads. Based on these results, it can be inferred that upon future extreme climates infiltration, heat gains will maintain an important role in additional annual cooling loads. At lower infiltration levels, the impacts of infiltration rate rises on annual cooling load increases would be even more obvious.

Finally, based on the benefit validation results of coupled variable optimizations it can be deduced that the simultaneous optimizations of different envelope design variables can realize their heat gain control and energy-saving benefits comprehensively. Although the collective employments of various optimization measures cannot simply lead to the superposition of energy-saving effects by respective variable optimizations, remarkable comprehensive energy-saving benefits can still be achieved.

Therefore, focusing on key design variables, the main energy-saving optimization strategies found upon future extreme climates in the subtropical climate regions can be mainly summarized as follows:

Firstly, low-performance insulation materials (vermiculite-type) should be avoided; economic insulation retrofitting with comparatively medium- and high-performance insulation (plastic- and rock wool-types) should be more readily considered. For the medium- and long-future-term scenarios, comparatively medium and high material thicknesses would be suitable, respectively.

Afterwards, for energy savings through WWR adjustments, the large WWRs in both eastern and western facades should be avoided as much as possible, while adequate daylight introduced through northern and southern facade openings are more favored. In order to ensure an energy-saving effect, only appropriate opening them proportionally to meet the daylight needs can be considered, but excessive WWRs should also be avoided.

Moreover, in response to future extreme climates, enough attention should also be paid to strictly control of the envelope infiltration rates to avoid unnecessary additional cooling loads. Since at lower infiltration levels the cooling load impacts on infiltration rate rises tend to be more obvious, the infiltration rate should be controlled as far as possible for attaining the lowest level.

Finally, the optimizations of various design variables can be applied simultaneously to improve both the envelope thermal properties and the infiltration performances, therefore achieving remarkable and comprehensive energy-saving benefits for subtropical-area container buildings in future extreme climate conditions.

6. Conclusions and Outlook

In response to the increasing container building boom in cities, and the world's more and more serious extreme climate change, the problem of energy consumption of such a typical small-scale building typology has become increasingly prominent. To mitigate energy burdens brought by such phenomenon, this study predicted key future climates scenarios on the basis of the present TMY. Though detailed simulation works over typical contemporary container housing prototypes tuned by key design factors, the actual cooling energy impacts of envelope properties in subtropical areas have been overall investigated with regards to future climate conditions. This work provides meaningful insight into the energy and thermophysical behaviors of the container carried housing typology in subtropical regions, in the face of upcoming extreme climate scenarios. Among such warm winter and hot summer climate zones or similar climate regions, the main conclusions for a green container housing design of future are as follows:

1. Firstly, even in subtropical regions, climate extremities are relatively significant (temperature increases, relative humidity decreases), especially the maximum summer outdoor temperature rises significantly (about 1 °C). Further into the future, this phenomenon will not be obviously alleviated. Accordingly, the indoor and outdoor surface temperatures, as well as the corresponding cooling loads of the container housing, also increased clearly (about 0.5 °C). The enlarging indoor and outdoor temperature disparity (opening and

closing period of air conditioning) caused by more extreme external high temperatures can be accounted for as the critical factor of extra cooling energy consumption.

2. Secondly, the heat gains from envelopes and hot air infiltration are both key design factors of cooling energy increments for the container carrier buildings in future extreme climate conditions. In response to the increasingly overheated outdoor temperature, special attention should be paid to the selection of external insulation materials, thicknesses, and WWRs, as well as the control of air infiltration rates.

3. Moreover, compared with expanded pearl- and vermiculite-type insulation materials, plastic- and mineral wool-type ones have better energy-saving performance in response to future climate extremes and therefore are more worthy of consideration. Thinner plastic-type insulation (70~80 mm) can achieve the same energy-saving effect as slightly thicker mineral wool-type materials (80~90 mm), so is more recommended for medium-future scenarios. For long-term-future climate scenarios, you may need thicker choices (~100 mm) to ensure enough insulation performance. Meanwhile, regardless of recent or long-term climate extreme predictions, WWRs and air infiltration rates should always be given enough attention. Especially for more sensitive eastern and western façades, it is necessary to avoid excessive size openings but more moderate WWRs, while larger WWRs in the northern and southern directions can be considered to increase indoor daylighting. In addition, compared with higher infiltration rates, it is necessary to strictly control the infiltration heat gains at lower infiltration rates to ensure more limited cooling energy consumption.

4. Finally, the simultaneous optimizations of different envelope design variables in a collective manner can realize their heat gain control and energy-saving benefits comprehensively, and therefore should be recommended for subtropical-area container buildings in future extreme climate conditions.

This study can provide a valuable guide for decision-making on energy-efficient designs, prefabrication, or refurbishments of container building, among the tested subtropical region or similar climate zones.

Based on this research, subsequent research can further explore the impacts of different natural ventilation modes on the above energy-saving design measures, and how to achieve better daylighting effects under this energy-saving premise, etc.

Author Contributions: Conceptualization, H.S. and X.G.; methodology, H.S. and X.G.; software, X.G.; validation, H.S. and X.G.; formal analysis, H.S. and X.G.; investigation, H.S. and X.G.; resources, H.S., S.W. and Z.F.; data curation, X.G.; writing—original draft preparation, H.S. and X.G.; writing—review and editing, H.S., S.W. and Z.F.; visualization, X.G.; supervision, H.S. and Z.F.; project administration, H.S. and S.W.; funding acquisition, S.W. All authors have read and agreed to the published version of the manuscript.

Funding: This work was supported by Foundation and Applied Basic Research Fund project of Guangdong Province (NO:2019A1515110998, Research on Architectural Design Optimization under High Humidity Weather of "Hui Nan Tian" in Guangdong Region) and by Guangdong University Innovation Team of Guangdong Provincial Department of Education (NO. 2021KCXTD027 Carbon-neutral smart energy key technology and application innovation team).

Institutional Review Board Statement: Not applicable.

Informed Consent Statement: Not applicable.

Data Availability Statement: Data will be available upon request.

Conflicts of Interest: The authors declare no conflict of interest.

Abbreviations

ACH	Air Change per Hour
GHG	Greenhouses Gas
HVAC	Heating, Ventilation and Air Conditioning
IPCC	Intergovernmental Panel on Meteorological Change

IWEC	International Weather for Energy Calculation
NZECBs	Nearly Zero-Energy Container Buildings
PCMs	Phase-Change Materials
PU	Rigid polyurethane foam
RY	Reference Year
TEU	Twenty Feet Equivalent Unit
TMY	Typical Meteorological Year
VIPs	Vacuum Insulated Panels
WWRs	window-to-wall ratio

References

1. Ministry of Transport of the People's Republic of China. 2019 Waterway Freight Traffic. Available online: https://www.mot.gov.cn (accessed on 1 November 2022).
2. Peng, C. Application of prefabricated building in emergency rescue project construction Taking—Wuhan Huoshenshan Hospital Project as an example. *IOP Conf. Ser. Earth Environ. Sci.* **2021**, *742*, 012005. [CrossRef]
3. JAMES & MAU. Infinski Manifesto House. Available online: https://jamesandmau.com/projects/infiniski-manifesto-house (accessed on 3 November 2022).
4. Trinity Buoy Wharf. Container City 2. Available online: https://www.trinitybuoywharf.com/architecture/container-city-2 (accessed on 3 November 2022).
5. TEMPOHOUSING. KEETWONEN. Available online: http://www.tempohousing.com/projects/keetwonen/ (accessed on 3 November 2022).
6. ARCHNET. Container Temporary Housing. Available online: https://www.archnet.org/sites/6965 (accessed on 3 November 2022).
7. FIFA WORLD CUP Qatar. Stadium 974. 2022. Available online: https://www.qatar2022.qa/en/tournament/stadiums/stadium-974 (accessed on 5 November 2022).
8. FIFA WORLD CUP Qatar. My Hayya and My Accommodation. 2022. Available online: https://www.qatar2022.qa/book/en/fan-Villages (accessed on 5 November 2022).
9. Le Quéré, C.; Andrew, R.M.; Canadell, J.G.; Sitch, S.; Korsbakken, J.I.; Peters, G.P.; Manning, A.C.; Boden, T.A.; Tans, P.P.; Houghton, R.A.; et al. Global carbon budget 2016. *Earth Syst. Sci. Data* **2016**, *8*, 605–649. [CrossRef]
10. Energy Consumption Special Committee of China Building Energy Conservation Association. China Building Energy Consumption Research Report 2022. *Build. Energy Effic.* **2021**, *49*, 1–6. (In Chinese)
11. Ministry of Ecology and Environment the People's Republic of China. President Xi Jinping Delivered an Important Speech at the General Debate of the 75th United Nations General Assembly. Available online: https://www.mee.gov.cn/ywdt/szyw/202009/t20200923_799947.shtml (accessed on 6 November 2022).
12. Kristiansen, A.B.; Ma, T.; Wang, R.Z. Perspectives on industrialized transportable solar powered zero energy buildings. *Renew. Sustain. Energy Rev.* **2019**, *108*, 112–124. [CrossRef]
13. Jia, J.; Gao, F.; Cheng, Y.; Wang, P.; Ei-Ghetany, H.H.; Han, J. A comparative study on thermoelectric performances and energy savings of double-skin photovoltaic windows in cold regions of China. *Sol. Energy* **2020**, *206*, 464–472. [CrossRef]
14. Cuce, E.; Riffat, S.B.; Young, C.H. Thermal insulation, power generation, lighting and energy saving performance of heat insulation solar glass as a curtain wall application in Taiwan: A comparative experimental study. *Energy Convers. Manag.* **2015**, *96*, 31–38. [CrossRef]
15. Xu, S.; Liao, W.; Huang, J.; Kang, J. Optimal PV cell coverage ratio for semi-transparent photovoltaics on office building facades in central China. *Energy Build.* **2014**, *77*, 130–138. [CrossRef]
16. Gonçalves, J.E.; van Hooff, T.; Saelens, D. Understanding the behaviour of naturally-ventilated BIPV modules: A sensitivity analysis. *Renew. Energy* **2020**, *161*, 133–148. [CrossRef]
17. Yu, G.; Yang, H.; Luo, D.; Cheng, X.; Ansah, M.K. A review on developments and researches of building integrated photovoltaic (BIPV) windows and shading blinds. *Renew. Sustain. Energy Rev.* **2021**, *149*, 111355. [CrossRef]
18. Salata, F.; Falasca, S.; Ciancio, V.; Curci, G.; Grignaffini, S.; de Wilde, P. Estimating building cooling energy demand through the Cooling Degree Hours in a changing climate: A modeling study. *Sustain. Cities Soc.* **2021**, *76*, 103518. [CrossRef]
19. Ascione, F.; De Masi, R.F.; Gigante, A.; Vanoli, G.P. Resilience to the climate change of nearly zero energy-building designed according to the EPBD recast: Monitoring, calibrated energy models and perspective simulations of a Mediterranean nZEB living lab. *Energy Build.* **2022**, *262*, 112004. [CrossRef]
20. Schiavoni, S.; Sambuco, S.; Rotili, A.; D'Alessandro, F.; Fantauzzi, F. A nZEB housing structure derived from end of life containers: Energy, lighting and life cycle assessment. *Build. Simul.* **2017**, *10*, 165–181. [CrossRef]
21. Kristiansen, A.; Satola, D.; Lee, K.; Zhao, B.; Ma, T.; Wang, R.; Gustavsen, A.; Novakovic, V. Feasibility study of an off-grid container unit for industrial construction. *Sustain. Cities Soc.* **2020**, *61*, 102335. [CrossRef]
22. Satola, D.; Kristiansen, A.; Houlihan-Wiberg, A.; Gustavsen, A.; Ma, T.; Wang, R. Comparative life cycle assessment of various energy efficiency designs of a container-based housing unit in China: A case study. *Build. Environ.* **2020**, *186*, 107358. [CrossRef]
23. Trancossi, M.; Cannistraro, G.; Pascoa, J. Thermoelectric and solar heat pump use toward self sufficient buildings: The case of a container house. *Therm. Sci. Eng. Prog.* **2020**, *18*, 100509. [CrossRef]

24. Tanyer, A.M.; Tavukcuoglu, A.; Bekboliev, M. Assessing the airtightness performance of container houses in relation to its effect on energy efficiency. *Build. Environ.* **2018**, *134*, 59–73. [CrossRef]
25. Taleb, H.; Elsebaei, M.; EL-Attar, M. Enhancing the sustainability of shipping container homes in a hot arid region: A case study of Aswan in Egypt. *Archit. Eng. Des. Manag.* **2019**, *15*, 459–474. [CrossRef]
26. Nan, X.; Yan, H.; Wu, R.; Shi, Y.; Bao, Z. Assessing the thermal performance of living wall systems in wet and cold climates during the winter. *Energy Build.* **2020**, *208*, 109680. [CrossRef]
27. Liebman-Pelaez, M.; Kongoletos, J.; Norford, L.K.; Reinhart, C. Validation of a building energy model of a hydroponic container farm and its application in urban design. *Energy Build.* **2021**, *250*, 111192. [CrossRef]
28. Koke, J.; Schippmann, A.; Shen, J.; Zhang, X.; Kaufmann, P.; Krause, S. Strategies of Design Concepts and Energy Systems for Nearly Zero-Energy Container Buildings (NZECBs) in Different Climates. *Buildings* **2021**, *11*, 364. [CrossRef]
29. Energyplus. Energyplus. Available online: https://energyplus.net (accessed on 8 November 2022).
30. *GB50176-2016*; Thermal Design Code for Civil Building. Ministry of Housing and Urban-Rural Development of the People's Republic of China: Beijing, China, 2016.
31. *JGJ 75-2012*; Design Standard for Energy Efficiency of Residential Buildings in Hot Summer and Warm Winter Zone. Ministry of Housing and Urban-Rural Development of the People's Republic of China: Beijing, China, 2012.
32. *CECS334:2013*; Technical Specification for Modular Freight Container Building. China Association of Engineering Construction: Beijing, China, 2013.
33. *JGJ 449-2018*; Standard for Green Performance Calculation of Civil Buildings. Ministry of Housing and Urban-Rural Development of the People's Republic of China: Beijing, China, 2018.
34. *JGJ 144-2019*; Technical Standard for External Thermal Insulation on Walls. Ministry of Housing and Urban-Rural Development of the People's Republic of China: Beijing, China, 2019.
35. Cheng, P.L.; Li, X. Air infiltration rates in the bedrooms of 202 residences and estimated parametric infiltration rate distribution in Guangzhou, China. *Energy Build.* **2018**, *164*, 219–225. [CrossRef]
36. Belcher, S.; Hacker, J.; Powell, D. Constructing design weather data for future climates. *Build. Serv. Eng. Res. Technol.* **2005**, *26*, 49–61. [CrossRef]
37. Dias, J.B.; da Graca, G.C.; Soares, P.M.M. Comparison of methodologies for generation of future weather data for building thermal energy simulation. *Energy Build.* **2020**, *206*, 109556. [CrossRef]
38. Shen, P. Impacts of climate change on US building energy use by using downscaled hourly future weather data. *Energy Build.* **2017**, *134*, 61–70. [CrossRef]
39. Xu, X.; Li, H.; Yang, L.; Yu, J. Prediction of future building energy consumption under climate change. *Acta Energ. Sol. Sin.* **2018**, *39*, 1359–1366.
40. Hietaharju, P.; Pulkkinen, J.; Ruusunen, M.; Louis, J.-N. Near- and medium-term hourly morphed mean and extreme future temperature datasets for Jyväskylä, Finland, for building thermal energy demand simulations. *Data Brief* **2021**, *37*, 107209. [CrossRef]
41. Pachauri, R.K.; Allen, M.R.; Barros, V.R.; Broome, J.; Cramer, W.; Christ, R.; Church, J.A.; Clarke, L.; Dahe, Q.; Dasgupta, P.; et al. *Comprehensive Report on Climate Change of 2014*; Intergovernmental Panel on Climate Change: Copenhagen, Denmark, 2014.
42. University of Southampton Energy & Climate Change. Climate Change World Weather File Generator for World-Wide Weather Data—CCWorldWeatherGen. Available online: http://www.energy.soton.ac.uk/ccworldweathergen (accessed on 10 November 2022).
43. Wan, K.K.; Li, D.H.; Pan, W.; Lam, J.C. Impact of climate change on building energy use in different climate zones and mitigation and adaptation implications. *Appl. Energy* **2012**, *97*, 274–282. [CrossRef]
44. U.S. Department of Energy Office of Energy Efficiency & Renewable Energy. EnergyPlus Turns 20! Available online: https://www.energy.gov/eere/buildings/articles/energyplus-turns-20 (accessed on 15 December 2022).